Current Biology, Volume *27*

Supplemental Information

A Moving Source of Matrix Components Is Essential for *De Novo* Basement Membrane Formation

Yutaka Matsubayashi, Adam Louani, Anca Dragu, Besaiz J. Sánchez-Sánchez, Eduardo Serna-Morales, Lawrence Yolland, Attila Gyoergy, Gema Vizcay, Roland A. Fleck, John M. Heddleston, Teng-Leong Chew, Daria E. Siekhaus, and Brian M. Stramer

Figure S1

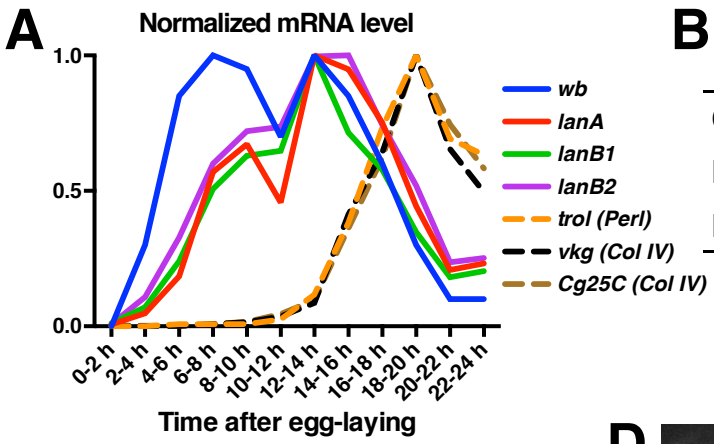

B

	Embryonic lethality	
Control	8/53	(15%)
LanA mut	50/52	(96%)
LanA mut + LanA-GFP	2/59	(3%)

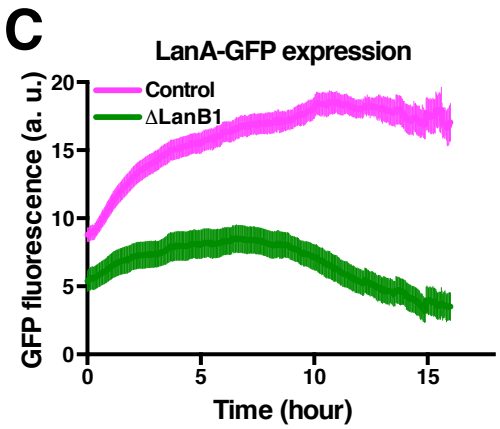

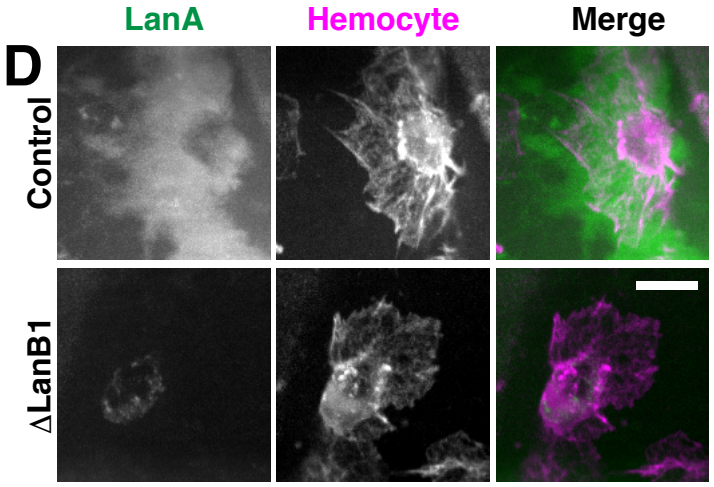

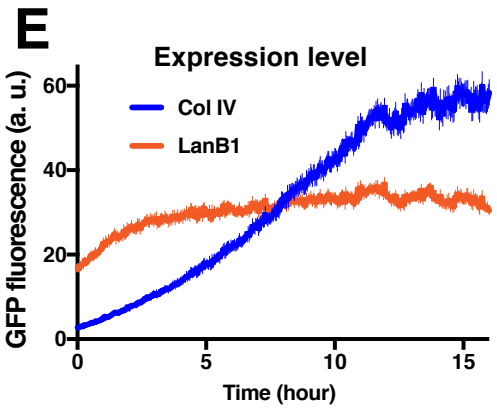

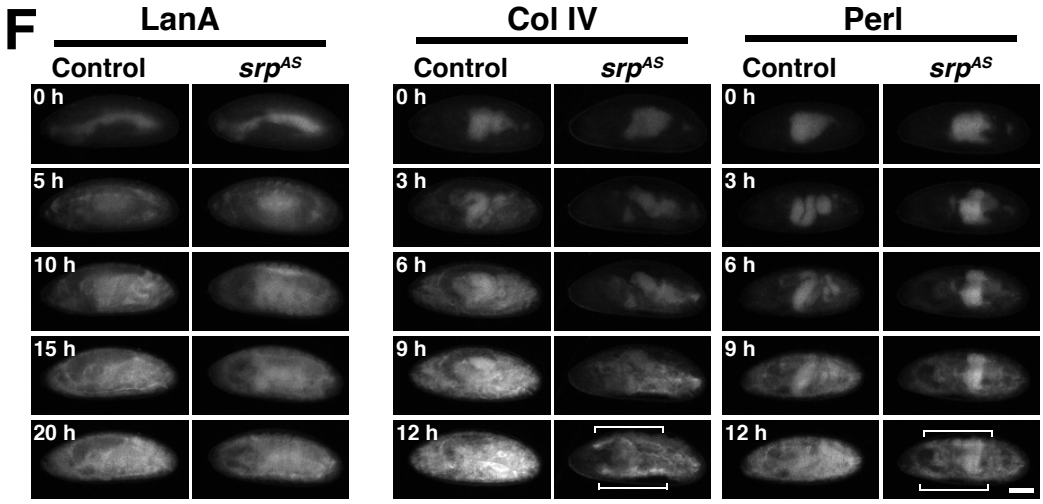

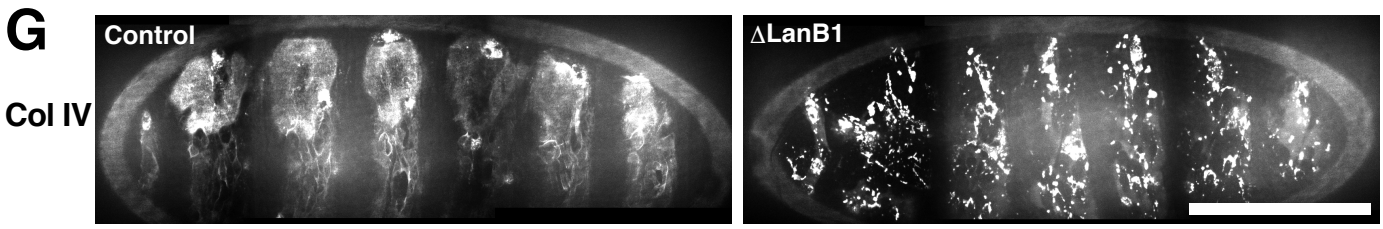

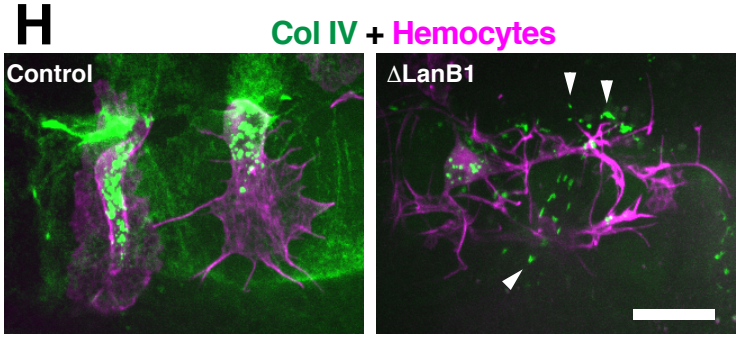

Figure S2

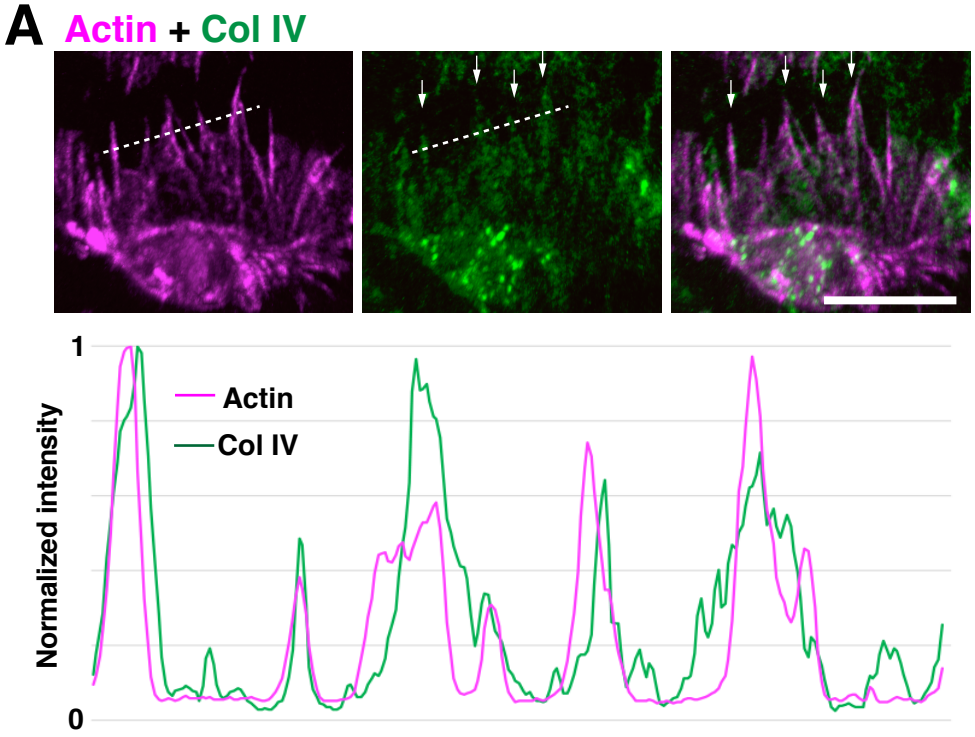
A
Actin + Col IV
1
0
Normalized intensity
Actin
Col IV

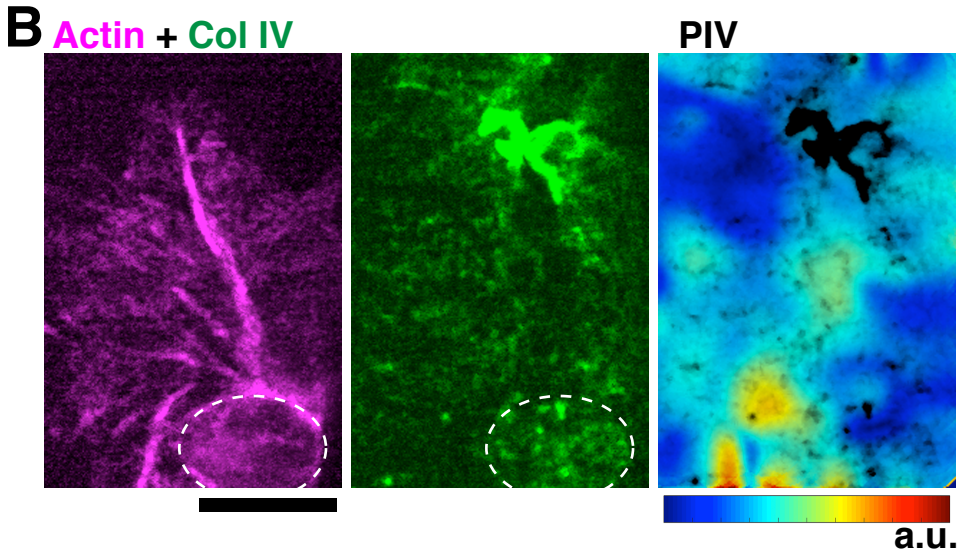
B
Actin + Col IV
PIV
a.u.

Figure S3

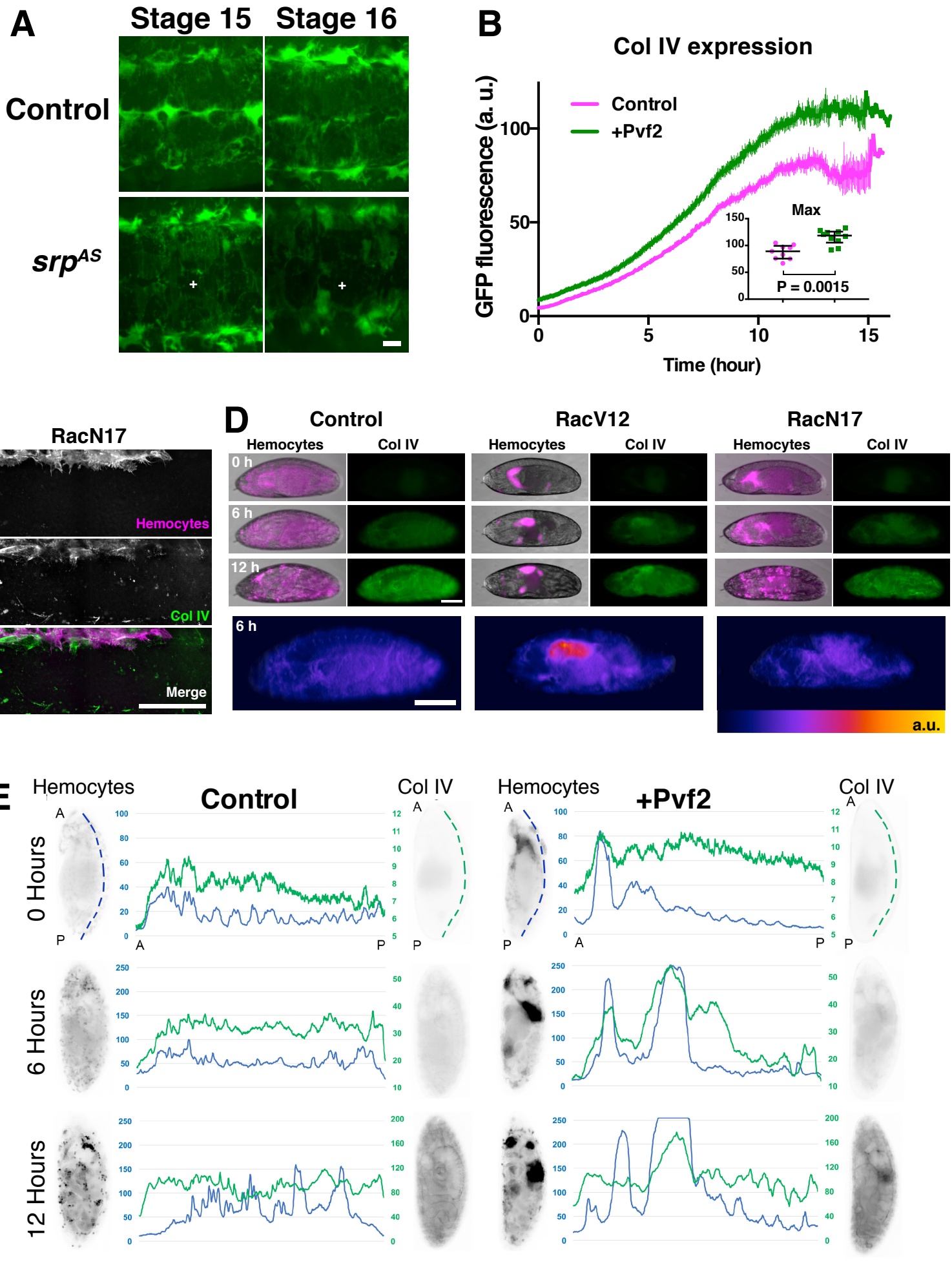
A
Stage 15
Stage 16
Control
srpAS
B
Col IV expression
Control
+Pvf2
GFP fluorescence (a. u.)
Time (hour)
Max
P = 0.0015
C
RacN17
Hemocytes
Col IV
Merge
D
Control
RacV12
RacN17
Hemocytes
Col IV
0 h
6 h
12 h
a.u.
E
Control
+Pvf2
0 Hours
6 Hours
12 Hours

Figure S4

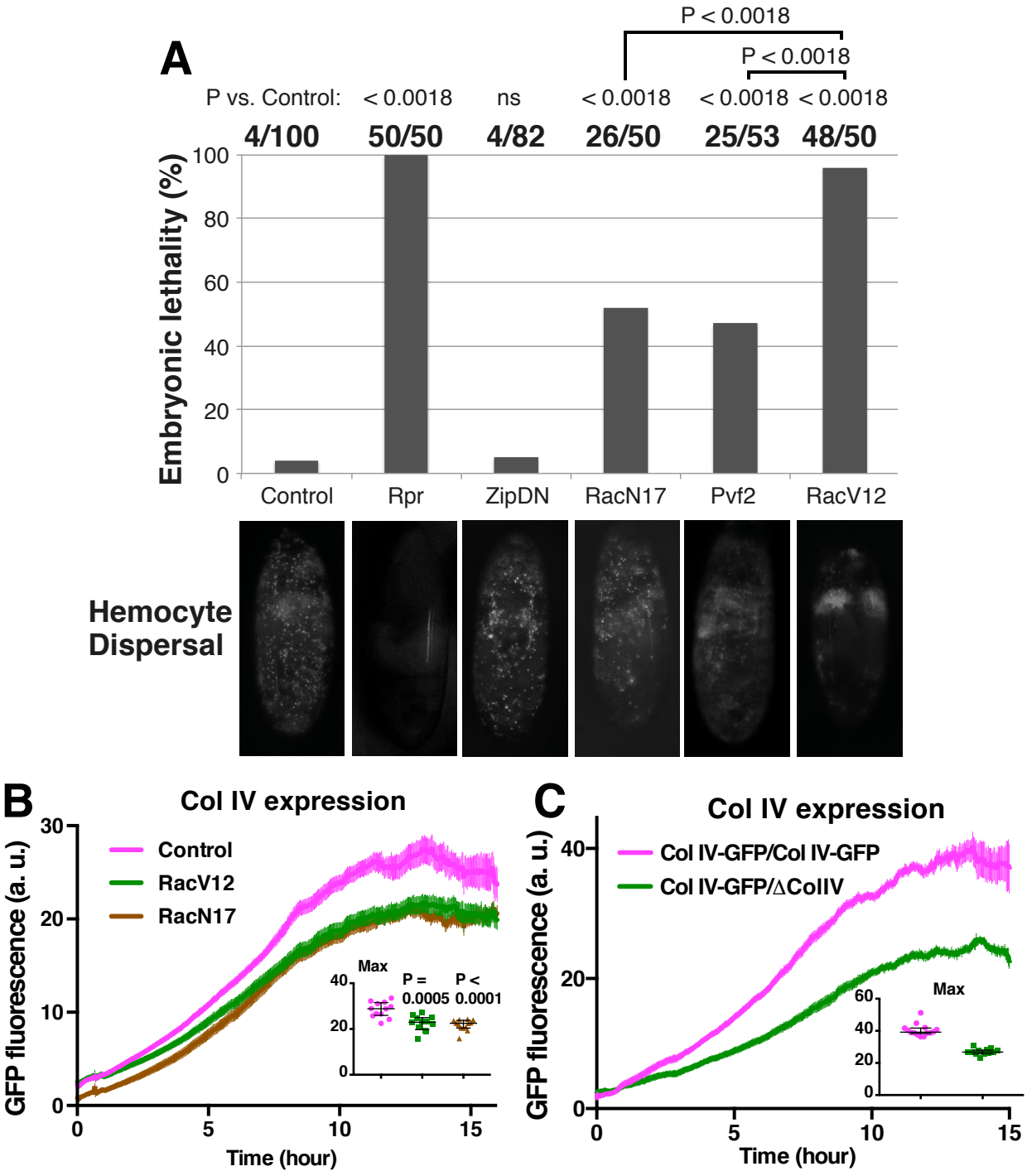
A
P < 0.0018
P < 0.0018
P vs. Control:
< 0.0018
ns
< 0.0018
< 0.0018
< 0.0018
4/100
50/50
4/82
26/50
25/53
48/50
Embryonic lethality (%)
100
80
60
40
20
0
Control
Rpr
ZipDN
RacN17
Pvf2
RacV12
Hemocyte Dispersal
B
Col IV expression
Control
RacV12
RacN17
GFP fluorescence (a. u.)
30
20
10
0
0
5
10
15
Time (hour)
Max
40
20
0
P = 0.0005
P < 0.0001
C
Col IV expression
Col IV-GFP/Col IV-GFP
Col IV-GFP/ΔColIV
GFP fluorescence (a. u.)
40
20
0
0
5
10
15
Time (hour)
Max
60
40
20
0

Figure S1. Characterization of the levels and localization of BM components. Related to Figure 1.

(A) Developmental time-course of mRNA expression levels encoding the BM proteins. The RNAseq data was downloaded from modENCODE. Note that the expression of Laminin subunits (*wb, lanA, lanB1 and lanB2*, solid lines) precedes that of Collagen IV (*vkg* and *Cg25c*) and Perlecan (*trol*) (dashed lines).

(B) LanA-GFP rescues LanA mutant. Lethality of the embryos was quantified in the indicated genotypes. For each genotype, the results are shown in the format of (number of dead embryos) / (total number of embryos examined).

(C) Expression of LanA-GFP depends on LanB1. The fluorescence levels of LanA-GFP in Control (magenta) and ΔLanB1 (green) embryos was measured and plotted against time as in Figure 1C. Mean ± SEM.

(D) Confocal images of LanA-GFP (green) and hemocytes (magenta) in Control and ΔLanB1 embryos. Note that LanA-GFP is reduced and remaining LanA is not found outside hemocytes in ΔLanB1 embryos. Scale bar, 10 μm.

(E) The fluorescence levels of Col IV-GFP (blue) and LanB1-GFP (orange) was measured and plotted against time as in Figure 1C. Note that expression of LanB1-GFP precedes that of Col IV-GFP. Mean ± SEM.

(F) Time-lapse imaging of *Drosophila* embryos expressing GFP-tagged BM components in Control and srp^{AS} mutant embryos, in which hemocytes fail to develop. Note that due to its earlier expression, LanA imaging was started at embryonic stage 12, while Col IV and Perl imaging was started at stage 15. Scale bar, 100 μm. Brackets highlight fat body expression.

(G) Confocal images of Col IV in control and *lanB1* mutant (ΔLanB1) embryos. Note the large disorganised aggregations in the ΔLanB1 mutant. Scale bar, 100 μm.

(H) Confocal images of Col IV (green) and hemocytes (magenta) in Control and a *lanB1* mutant (ΔLanB1). Note that the Col IV aggregations (arrowheads) are outside hemocytes in the ΔLanB1 mutant. Scale bar, 10 μm.

Figure S2. Colocalization of actin with newly deposited Col IV and tracking BM deformation.
Related to Figure 2.

(A) Lattice light-sheet image of Col IV (green) and hemocyte actin (magenta). Graph highlights a linescan of Col IV and Actin revealing their colocalization (arrows).

(B) Time-lapse imaging by lattice light sheet microscopy of Col IV (green) and hemocyte actin (magenta). The right panel shows tracking of Col IV features by particle image velocimetry (PIV), which reveals rapid movements surrounding hemocyte lamellae in the developing basement membrane. Note the strong intracellular vesicles of Col IV within the hemocyte cell body (circle) with the remainder of the Col IV representing extracellular deposited protein. The heatmap is in arbitrary units and overlaid onto the Col IV image. Scale bars, 10 μm.

Figure S3. Examination of the distribution of BM components upon hemocyte perturbation.
Related to Figure 3.

(A) Localization of LanA in control and Srp^{AS} mutant embryos, which lack hemocytes. In the Srp^{AS} embryos, which lack hemocytes, gaps in the nascent Laminin sheet enlarge over time (cross). Scale bar, 10 μm.

(B) The fluorescence of Col IV-GFP in Control (magenta) and embryos overexpressing Pvf2 (green) was measured and plotted as in Figure 1C. Note that Pvf2 overexpression enhances the expression of Col IV-GFP. Mean ± SEM. Inset shows quantification of the maximum fluorescence in each single embryo. Bars in the inset indicate median ± interquartile range.

(C) Confocal images of hemocytes (magenta) and Col IV (green) in an embryo expressing RacN17 specifically in hemocytes. Col IV is mainly deposited around the aggregated hemocytes. Scale bar, 50 μm.

(D) Comparison of hemocyte developmental dispersal with expression levels of Col IV-GFP by widefield microscopy when hemocyte migration is affected by hemocyte-specific expression of RacV12 or RacN17. Bottom panels are heatmaps of Col IV expression. Scale bars, 100 μm.

(E) Comparison of hemocyte developmental dispersal with expression levels of Col IV-GFP by widefield microscopy in control and embryos overexpressing Pvf2. Graphs represent linescans of hemocytes (blue) and Col IV (green) within the highlighted regions.

Imaging was started at embryonic stage 12, which is prior to the induction of Col IV expression. Scale bar, 100 μm.

Figure S4. Quantification of embryonic lethality and Col IV expression levels upon hemocyte perturbation

Related to Figure 4.

(A) Hemocytes were killed off by hemocyte-specific expression of an apoptosis inducing protein, Reaper (Rpr). Alternatively, hemocyte migration was impaired by hemocyte-specific expression of dominant negative myosin II (ZipDN), dominant negative Rac (RacN17), constitutively active Rac (RacV12), or ubiquitous expression of Pvf2, and embryonic hemocyte distribution imaged by widefield microscopy. The percentage of embryos that failed to hatch in each genotype was quantified. Scale bar, 100μm.

(B) The fluorescence of Col IV-GFP in Control embryos (magenta) and those expressing RacV12 (green) or RacN17 (brown) in hemocytes was measured and plotted as in Figure 1C. Note that while RacN17 and RacV12 decrease Col IV levels to a similar extent, they are statistically different with regards to inducing embryonic lethality (see Figure S4B). Mean ± SEM. Inset shows quantification of the maximum fluorescence in each single embryo. Bars in the inset indicate median ± interquartile range.

(C) The fluorescence levels of Col IV-GFP in embryos homozygous for the Col IV-GFP trap (Col IV-GFP/Col IV-GFP, magenta) versus those with one copy of Col IV-GFP but heterozygous for the Col IV mutant (ΔColIV) was measured and plotted as in Figure 1C. Note that the reduction of Col IV levels when heterozygous for the ΔColIV mutation shows that there is no compensation for a missing allele. Mean ± SEM. Inset shows quantification of the maximum fluorescence in each single embryo. Bars in the inset indicate median ± interquartile range.

Table S1. Genotypes of the embryos used in each experiment

Related to Figures 1-4, S1-S4, and Movies S1-S4

Figure	Panel	Label	Genotype
Figure 1	A, B	No GFP	w^{1118}
		LanA	LanA-GFP
		Col IV	Col IV-GFP
		Perl	Perl-GFP
	C	LanA, Control	LanA-GFP
		LanA, srp^{AS}	LanA-GFP, srp^{AS}
		Col IV, Control	Col IV-GFP
		Col IV, srp^{AS}	Col IV-GFP; srp^{AS}
		Perl, Control	Perl-GFP
		Perl, srp^{AS}	Perl-GFP; srp^{AS}
	D, E		LanA-GFP, Col IV-GFP or Perl-GFP in either control or the homozygous mutant background as indicated
Figure 2	A	LanA	LanA-GFP, sn-Gal4, UAS-CheMoe
		LanB1	LanB1-GFP, srp-Gal4, UASChe-Moe
		Col IV	Col IV-GFP, srp-Gal4, UAS-Che-Moe
	B	LanA	LanA-GFP, sn-Gal4, UAS-CheMoe
		SecrGFP	e22c-Gal4, srp-3xmCherry/+; UAS-secrGFP/+
		Col IV	Col IV-GFP, srp-Gal4, UAS-CheMoe
		Perl	Perl-GFP; srp-Gal4, UAS-CheMoe
	C	SecrGFP	e22c-Gal4, srp-3xmCherry/+; UAS-secrGFP/+
		LanA	LanA-GFP, srp-3XmCherry/+
		Col IV	Col IV-GFP
	D, E		w^{1118}
	F, G		Col IV-GFP, srp-3xmCherry
Figure 3	A-C	Control	e22c-Gal4, srp-3xmCherry/+; LanA-GFP/+
		+Pvf2	e22c-Gal4, srp-3xmCherry/UAS-Pvf2; LanA-GFP/+
	D-F	Control	e22c-Gal4, Col IV-GFP/Col IV-GFP; srp-3XmCherry/+
		+Pvf2	e22c-Gal4, Col IV-GFP/Col IV-GFP, UAS-Pvf2; srp-3XmCherry/+
Figure 4	A		w^{1118}
	B	Control	w^{1118}
		+Pvf2	e22c-Gal4/UAS-Pvf2
	C-E	Control	repoCherry/+
		+Pvf2	E22cGal4/+; repoCherry/Pvf2
		RacV12	repoCherry, sn-Gal4, UAS-LifeAct-GFP/UAS-RacV12
		RacN17	repoCherry, sn-Gal4, UAS-LifeAct-GFP/UAS-RacN17
		ΔCol IV/+	E22cGal4, ΔCol IV /+; repoCherry/+
		ΔCol IV/+, +Pvf2	E22cGal4, ΔCol IV /+; repoCherry/Pvf2
	F	ΔCol IV/+	ΔCol IV/+
		RacN17	srp-Gal4, UAS-Red-Stinger/UAS-RacN17
		ΔCol IV/+; RacN17	ΔCol IV/+; sn-Gal4, UAS-Red-Stinger/N17
		ΔCol IV/ΔCol IV	ΔCol IV/ΔCol IV
		ΔLanB1/+	ΔLanB1/+
		ΔLanB1/+; RacN17	ΔLanB1/+; sn-Gal4, UAS-Red-Stinger/N17
		ΔLanB1/ΔLanB1	ΔLanB1/ΔLanB1
Figure S1	A	NA	NA
	B	Control	$lanA^{9-32}$/TM3
		LanA mut	$lanA^{9-32}$/$lanA^{MB01129}$
		LanA mut + LanA-GFP	$lanA^{9-32}$/ $lanA^{MB01129}$, LanA-GFP
	C, D	Control	Col IV-GFP
		ΔLanB1	Col IV-GFP, ΔLanB1
	E	Col IV	Col IV-GFP
		LanB1	LanB1-GFP/+
	F	LanA, Control	LanA-GFP
		LanA, srp^{AS}	LanA-GFP, srp^{AS}
		Col IV, Control	Col IV-GFP
		Col IV, srp^{AS}	Col IV-GFP; srp^{AS}

		Perl, Control	Perl-GFP
		Perl, *srp*^{AS}	Perl-GFP; *srp*^{AS}
	G	Control	Col IV-GFP
		ΔLanB1	Col IV-GFP, ΔLanB1
	H	Control	Col IV-GFP; sn-Gal4, UAS-CheMoe
		ΔLanB1	Col IV-GFP, ΔLanB1; sn-Gal4, UAS-CheMoe
Figure S2	A		Col IV-GFP, srp-Gal4, UAS-CheMoe; sn-Gal4, UAS-CheMoe
	B		Col IV-GFP, srp-Gal4, UAS-CheMoe; sn-Gal4, UAS-CheMoe
Figure S3	A	Control	LanA-GFP
		srp^{AS}	LanA-GFP, *srp*^{AS}
	B	Control	Col IV-GFP/Col IV-GFP, UAS-Pvf2; srp-3XmCherry/+
		+Pvf2	e22c-Gal4, Col IV-GFP/Col IV-GFP, UAS-Pvf2; srp-3XmCherry/+
	C, D	Control	Col IV-GFP, srp-Gal4, UAS-CheMoe/Col IV-GFP; sn-Gal4, UAS-CheMoe/+
		RacV12	Col IV-GFP, srp-Gal4, UAS-CheMoe/Col IV-GFP; sn-Gal4, UAS-CheMoe/UAS-RacV12
		RacN17	Col IV-GFP, srp-Gal4, UAS-CheMoe/Col IV-GFP; sn-Gal4, UAS-CheMoe/UAS-RacN17
	E	Control	Col IV-GFP/Col IV-GFP, UAS-Pvf2; srp-3XmCherry/+
		+Pvf2	e22c-Gal4, Col IV-GFP/Col IV-GFP, UAS-Pvf2; srp-3XmCherry/+
Figure S4	A	Control	srp-Gal4, UAS-Red-Stinger
		Rpr	srp-Gal4, UAS-Red-Stinger X UAS-Rpr
		ZipDN	srp-Gal4, UAS-Red-Stinger/UAS-ZipDN
		RacN17	srp-Gal4, UAS-Red-Stinger/UAS-RacN17
		Pvf2	E22cGal4/UAS-Pvf2;srp-3xmCherry/+
		RacV12	srp-Gal4, UAS-Red-Stinger/UAS-RacV12
	B	Control	Col IV-GFP, srp-Gal4, UAS-CheMoe/Col IV-GFP; sn-Gal4, UAS-CheMoe/+
		RacV12	Col IV-GFP, srp-Gal4, UAS-CheMoe/Col IV-GFP; sn-Gal4, UAS-CheMoe/UAS-RacV12
		RacN17	Col IV-GFP, srp-Gal4, UAS-CheMoe/Col IV-GFP; sn-Gal4, UAS-CheMoe/UAS-RacN17
	C	Col IV-GFP/Col IV-GFP	Col IV-GFP
		Col IV-GFP/ΔCol IV	Col IV-GFP/ΔCol IV
Movie S1		No GFP	*w*^{1118}
		Perl	Perl-GFP
		Col IV	Col IV-GFP
		LanA	LanA-GFP
Movie S2	Part 1		LanA-GFP, sn-Gal4, UAS-CheMoe
	Part 2		Col IV-GFP, srp-Gal4, UAS-Che-Moe
Movie S3	Part 1		srpGal4, UAS-LifeAct-GFP, srp3XmCherry
	Part 2, 3		Col IV-GFP, srp-3xmCherry
	Part 4		Col IV-GFP, srp-Gal4, UAS-CheMoe; sn-Gal4, UAS-CheMoe
Movie S4	Part 1	LanA	LanA-GFP, srp-3xmCherry
		Col IV	Col IV-GFP, srp-3xmCherry
	Part 2	Control	e22c-Gal4, srp-3xmCherry/+; LanA-GFP/+
		+Pvf2	e22c-Gal4, srp-3xmCherry/UAS-Pvf2; LanA-GFP/+
	Part 3	Control	e22c-Gal4, Col IV-GFP/Col IV-GFP; srp-3XmCherry/+
		+Pvf2	e22c-Gal4, Col IV-GFP/Col IV-GFP, UAS-Pvf2; srp-3XmCherry/+
	Part 4		e22c-Gal4, Col IV-GFP/Col IV-GFP, UAS-Pvf2; srp-3XmCherry/+
	Part 5	Control	Col IV-GFP/Col IV-GFP, UAS-Pvf2; srp-3XmCherry/+
		+Pvf2	e22c-Gal4, Col IV-GFP/Col IV-GFP, UAS-Pvf2; srp-3XmCherry/+